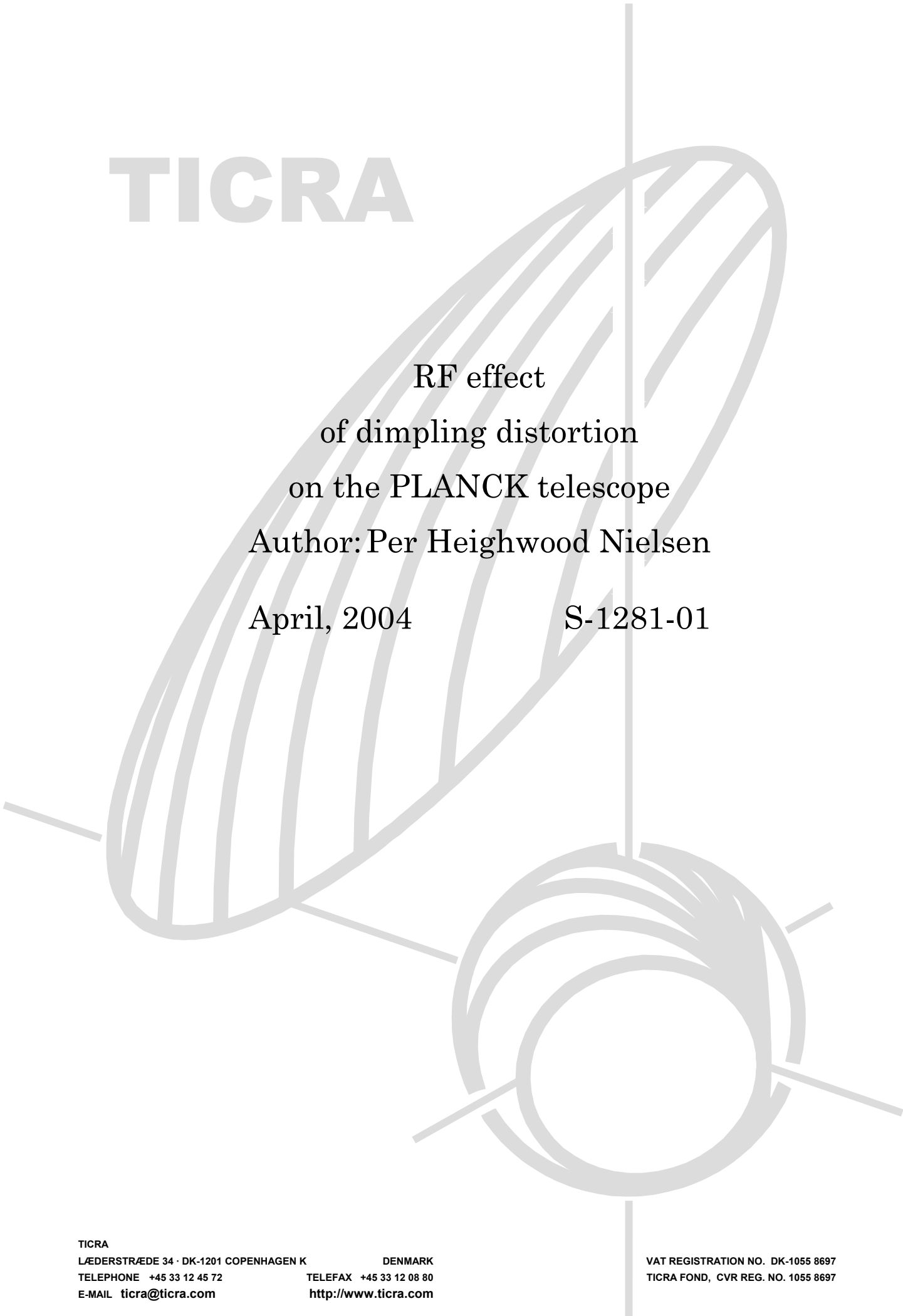


TICRA



RF effect
of dimpling distortion
on the PLANCK telescope
Author: Per Heighwood Nielsen

April, 2004

S-1281-01

TICRA

LÆDERSTRÆDE 34 · DK-1201 COPENHAGEN K

DENMARK

TELEPHONE +45 33 12 45 72

TELEFAX +45 33 12 08 80

E-MAIL ticra@ticra.com

<http://www.ticra.com>

VAT REGISTRATION NO. DK-1055 8697

TICRA FOND, CVR REG. NO. 1055 8697

TABLE OF CONTENTS

1. Introduction	1
2. RF performance of nominal mirrors	1
3. RF effects of dimpling surface errors	3
3.1 Distortions on primary mirror	3
3.2 Distortions on secondary mirror	8
3.3 Distortions on primary and secondary mirror	12
4. Frequency dependence	14
References	15

1. Introduction

The RF degradation of a periodic surface distortion structure known as dimpling is investigated in this report. The model of the dimpling distortion was presented in TICRA report S-801-05. Here the dimpling was here called core print-through and was bending upwards instead of downwards (concave) as for the present dimpling.

The RF performance of the distorted system is calculated with the GRASP9 program at the frequency 217 GHz for one of the horns (detectors), HFI217-1, and with two dimpling sizes. The horn is modelled as a simple Gaussian feed with the 30 dB taper at 21.8° as defined in ESA document SCI-PT-RS-07024, Chapter 5.2.1. The horn position is given in ALCATEL report H_P_3_ASPI_TN_0096

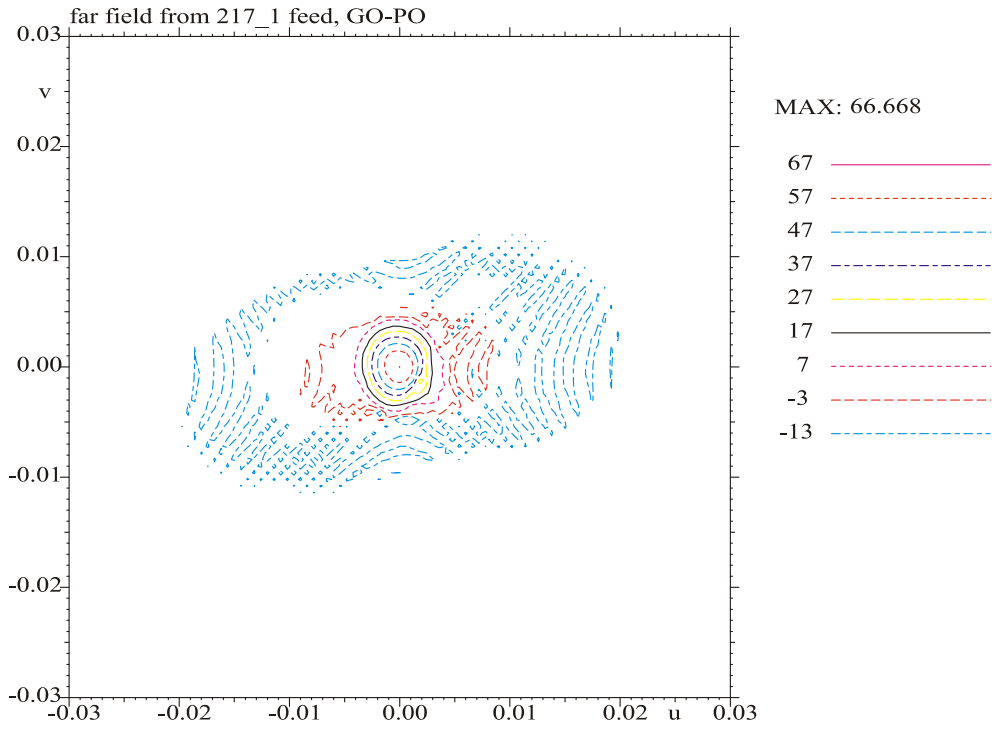
The geometry of the aplanatic design and the primary and secondary mirror is defined as in ESA document No. SCI-PT-RS-07024, but with new rim dimensions giving planar edge planes. In GRASP terminology the new dimensions are as follows:

Primary mirror rim size in x and y: 1500.00 mm * 1555.98 mm
and centre offset in x: 1038.85 mm

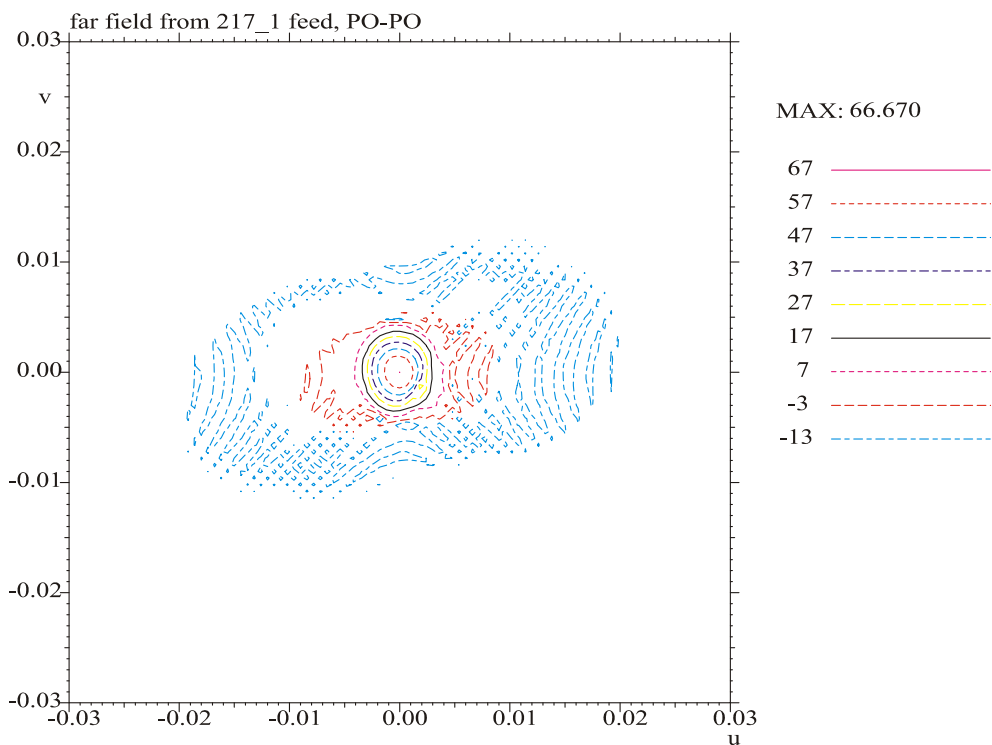
The RF performance of the nominal case without distortions is presented in Chapter 2, and the RF degradations due to the dimpling distortions with peaks of 10 μ and 2 μ on both the primary and the secondary mirror are presented in Chapter 3.

2. RF performance of nominal mirrors

The RF performance is calculated using Physical Optics, PO, on the primary mirror and Geometric Optics, GO, on the secondary mirror as for the 857 GHz case in TICRA Report S-801-05. The nominal far field is presented as contour curves in a UV grid, see Figure 2-1a where the centre is in the main beam direction. The contour curves are drawn for several field levels 10 dB, 20 dB, 30 dB, ..., 90 dB below the main peak of 66.67 dBi. For comparison, the RF performance using PO on the secondary mirror is shown in Figure 2-1b. The patterns are nearly identical with a peak difference of 0.002 dB only.



a) GO-PO



b) PO-PO

Figure 2-1 Far field from nominal mirrors.

3. RF effects of dimpling surface errors

The two-dimensional periodic structure of the dimpling surface distortion gives rise to grating lobes in the far field. The θ direction of the grating lobes, θ_{gr} , can be found by

$$\sin \theta_{gr} = \frac{2\lambda}{S_\ell} \quad \text{for } \phi=0^\circ + p*60^\circ \quad (3.1)$$

$$\sin \theta_{gr} = \frac{2\lambda}{S_\ell \sqrt{3}} \quad \text{for } \phi=30^\circ + p*60^\circ \quad (3.2)$$

where λ is the wavelength and S_ℓ is the projected side length in the aperture.

The pattern is calculated in the direction of the largest grating lobes, i.e. in the two cuts $\phi=0^\circ$ and 90° . The θ, ϕ direction is referred to an output co-ordinate system in the direction of the main beam, and with the $\phi=0^\circ$ plane in the antenna symmetry plane, see Figure 3-1b. The far field is also presented as contour curves in a UV grid, see Figure 3-1a, where the centre is in the main beam direction. The contour curves are drawn for several field levels 10 dB, 20 dB, 30 dB, ..., 90 dB below main peak.

The RF degradations are calculated for two different peaks of the dimpling distortion, 10μ and 2μ , on the primary- and the secondary mirror separately as described in Section 3.1 and Section 3.2, respectively. In Section 3.3 the total pattern is presented for 10μ dimpling on both the primary- and the secondary mirror

3.1 Distortions on primary mirror

The far field from the 10μ dimpling on the primary mirror is shown in a region up to 7.5° around the main beam in Figure 3-1a. The main beam is only reduced by 0.003 dB, but grating lobes are generated in a hexagonal grid around the main beam due to the periodic phase degradation. The largest grating lobe is in the $\phi = 90^\circ$ plane at $\theta = 2.25^\circ$ ($v=0.0393$) with a peak of 23.3 dBi, which is only 43 dB below the main beam peak. The most important grating lobes are also shown in the pattern cuts in Figure 3-1b. The θ direction of the grating lobes agrees very well with the equations (3.1) and (3.2) keeping in mind that the projected S_ℓ value is not 40 mm in the offset plane ($\phi=0^\circ$) but reduced to 33 mm. When the core print through peak is reduced to 2μ the grating lobes are reduced by $20\log(10\mu/2\mu)$ dB = 14 dB as shown in Figure 3-2.

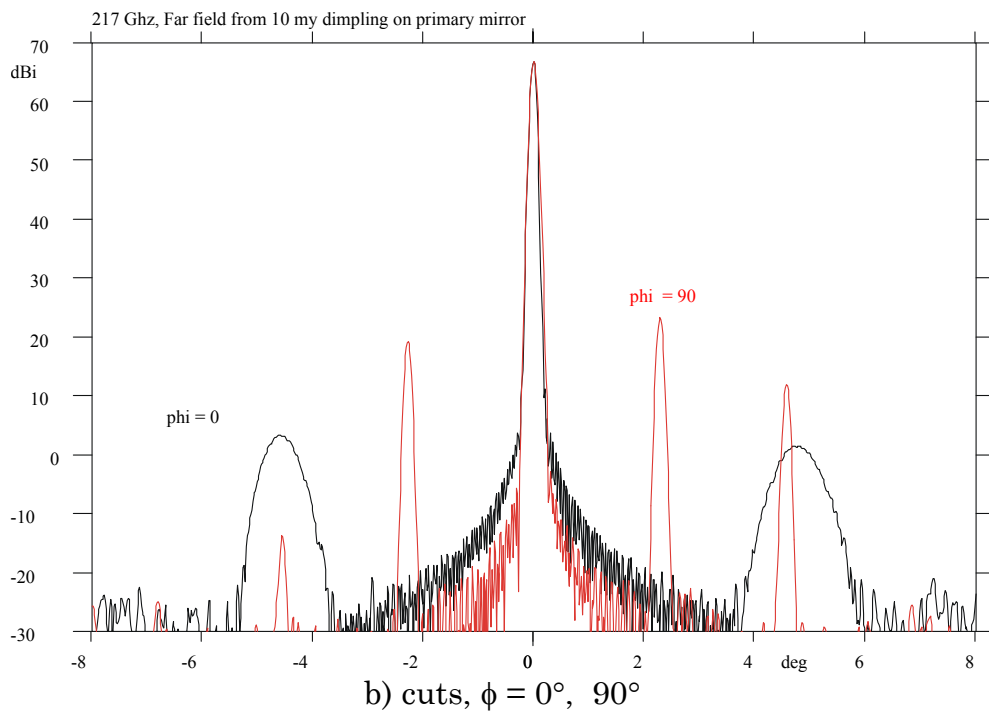
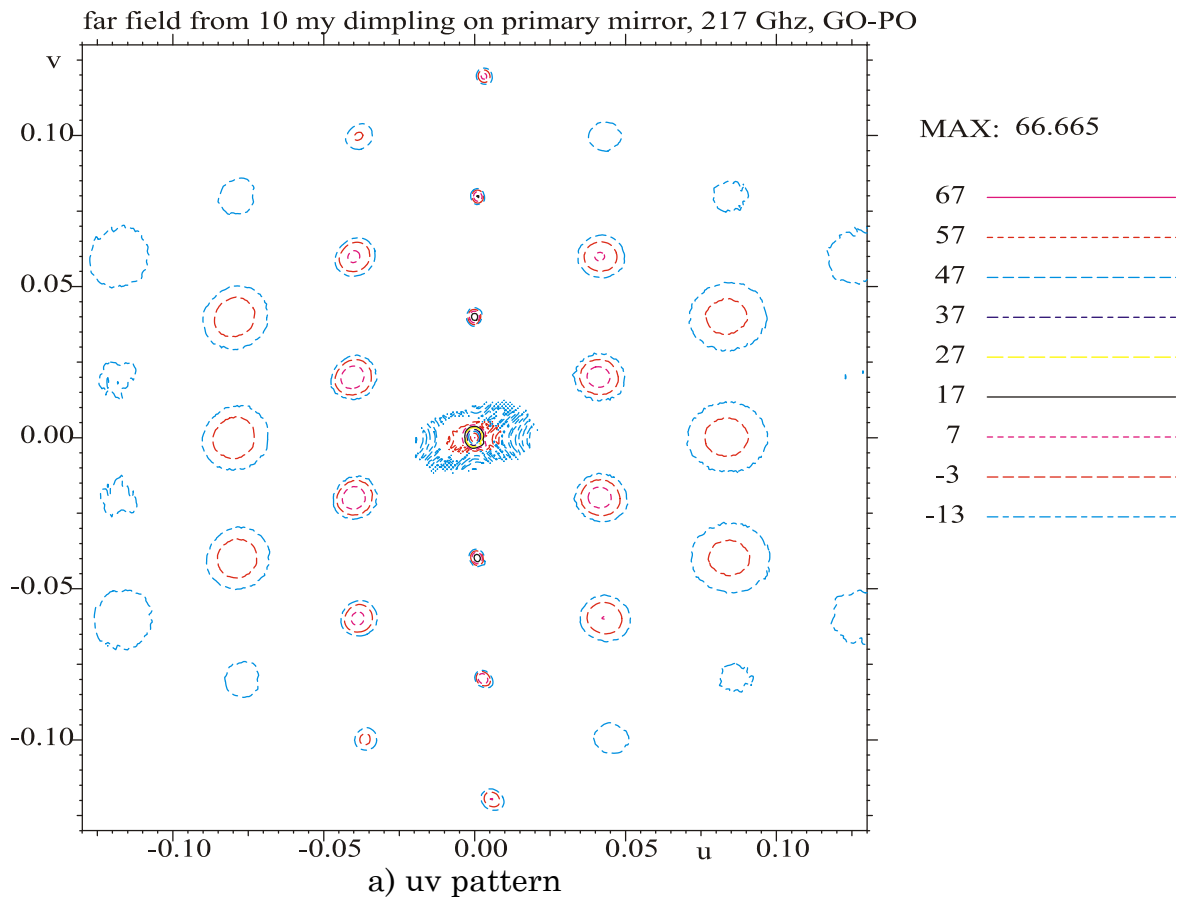


Figure 3-1 Far field from dimpling with 10μ peak on primary mirror. GO-PO

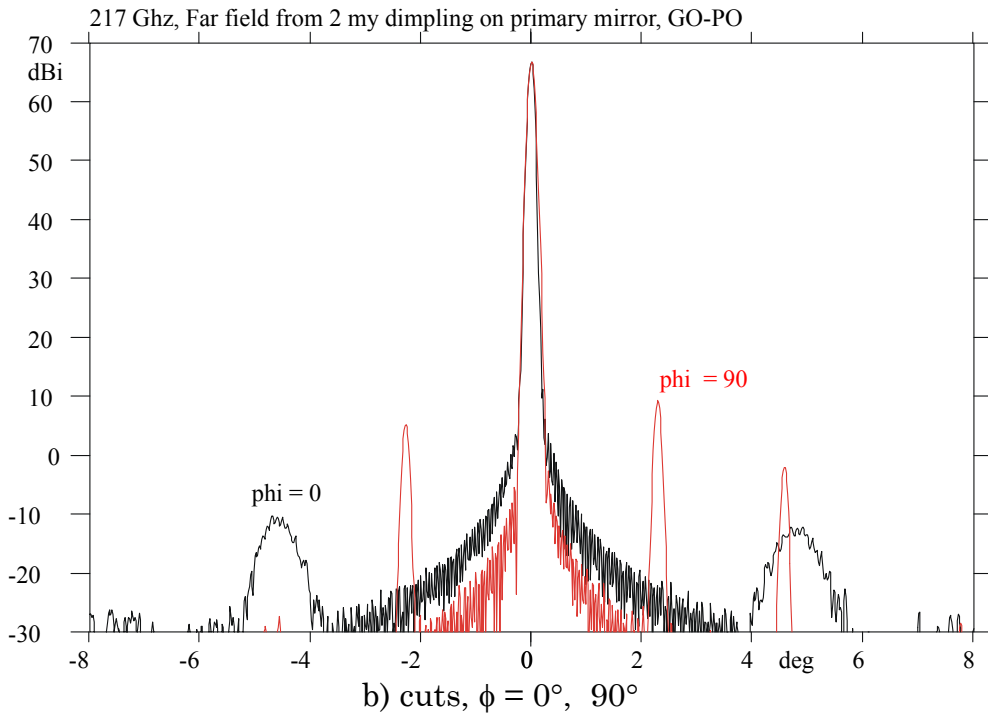
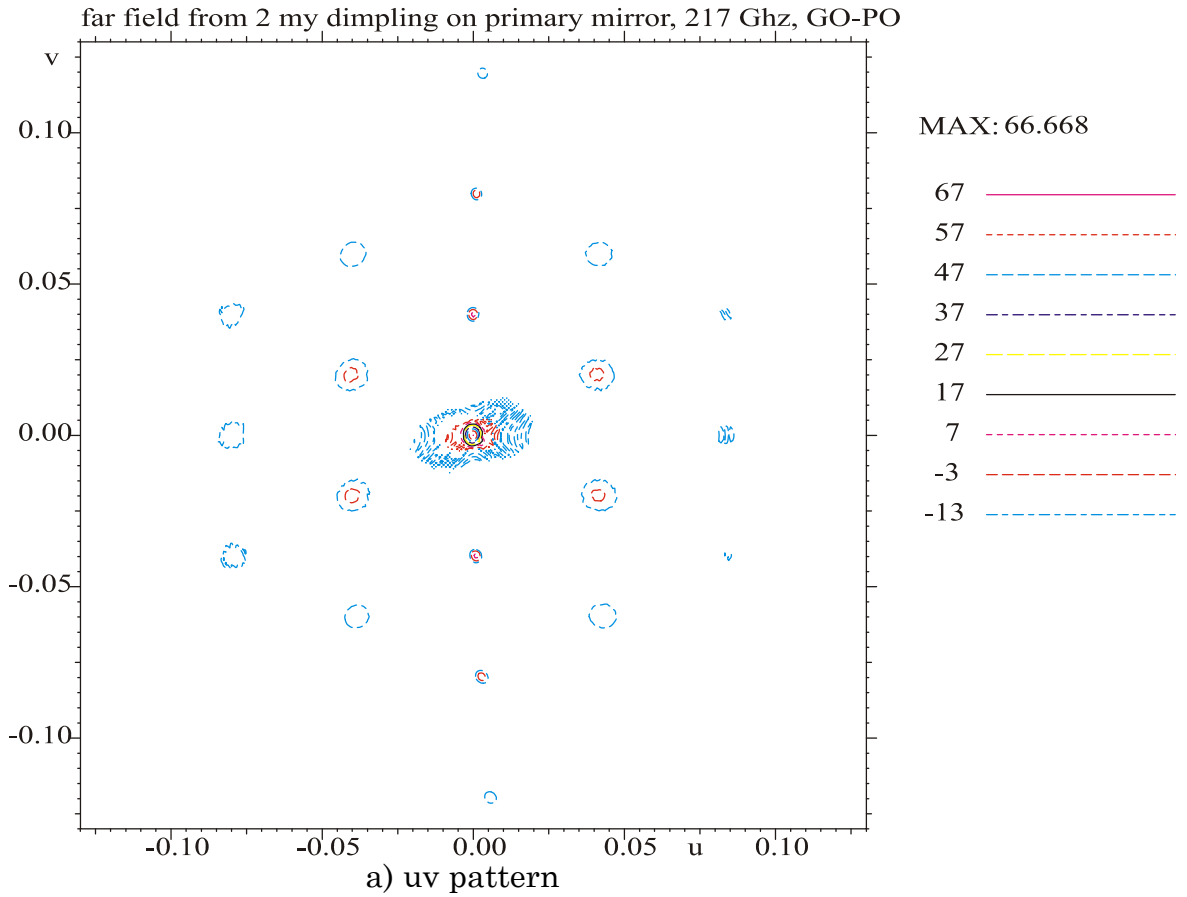


Figure 3-2 Far field from dimpling with 2 μ peak on primary mirror. GO-PO

In order to justify the use of GO on the secondary mirror the RF performance with 10μ dimpling on the primary mirror is recalculated using PO on the secondary mirror also. The patterns are shown in Figure 3-3. The shape of the patterns is identical to the patterns in Figure 3-1 from the GO-PO calculation. The only difference is in the peak level, where the PO-PO calculation gives a 0.002 dB larger result. But by inspecting the patterns for the nominal case see Figure 2-1, this peak increase is also found here, and therefore is not a consequence of the dimpling surface error.

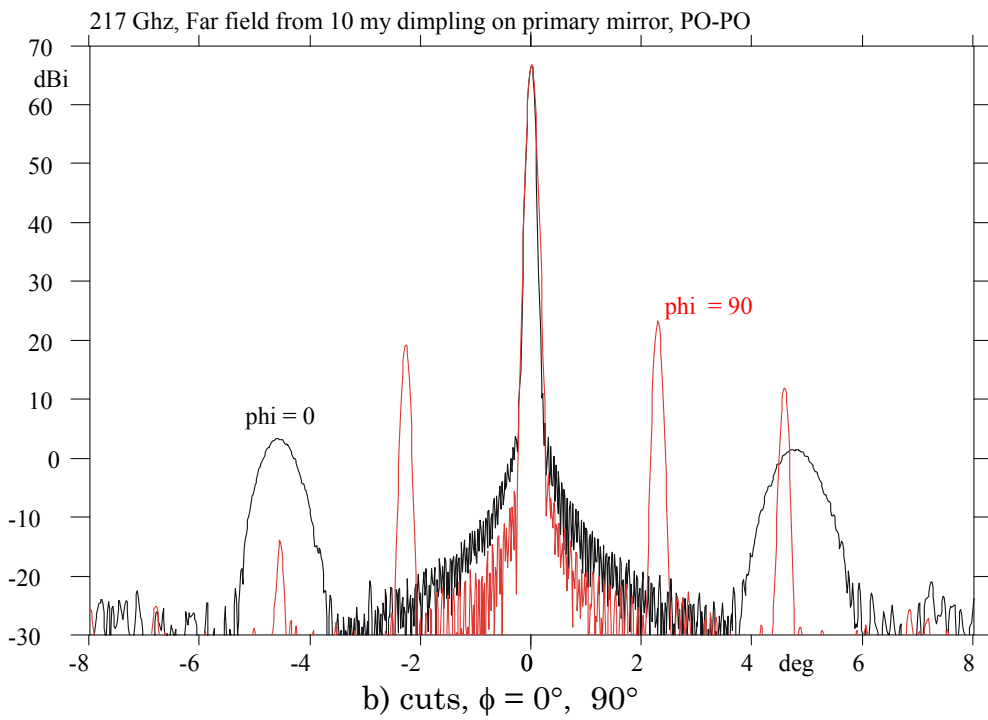
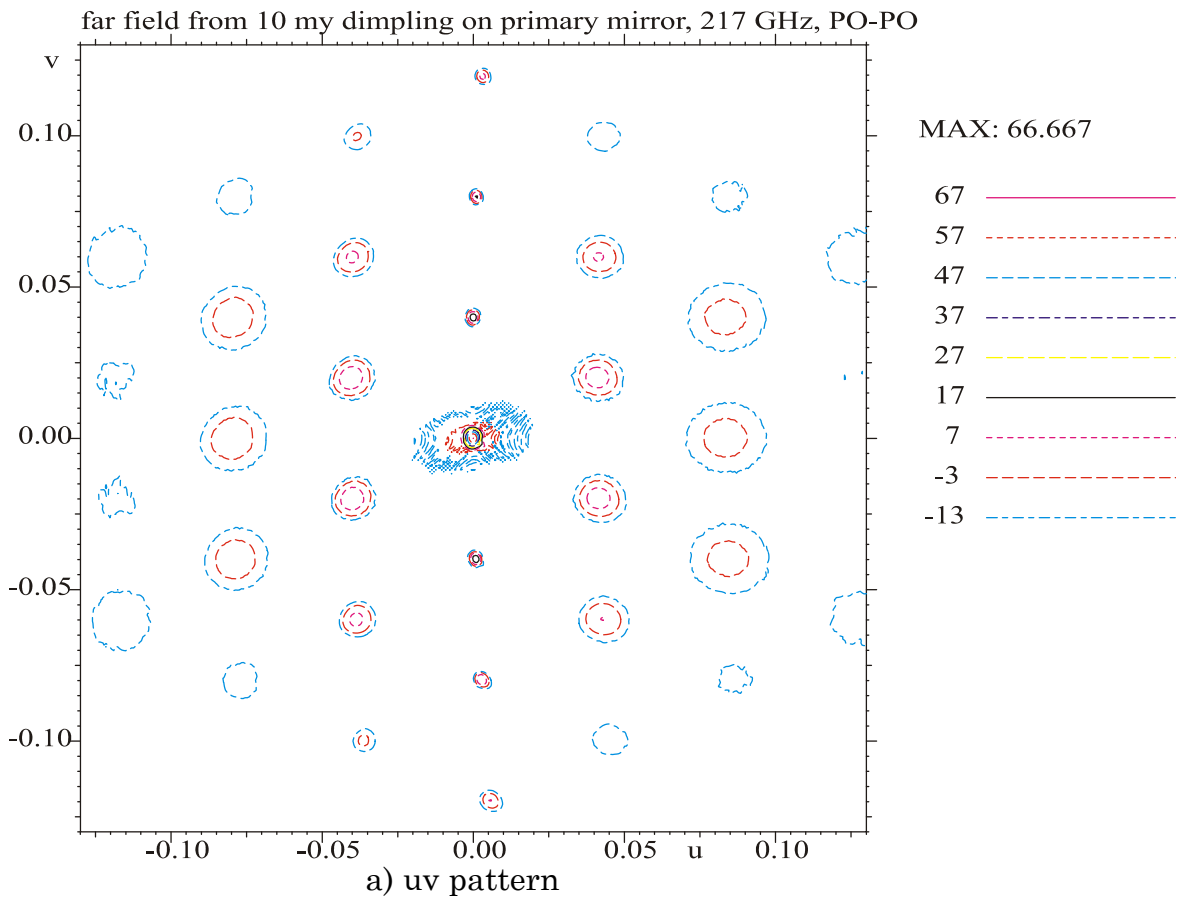


Figure 3-3 Far field from dimpling with 10 μ peak on primary mirror. PO-PO

3.2 Distortions on secondary mirror

The far field from the $10\ \mu$ dimpling on the secondary mirror is shown in Figure 3-4. The closer grating lobes in Figure 3-4a are due to the projection of the phase degradation from the triangular dimpling up to the primary mirror aperture. Thereby, the distance between the triangles is increased in the x direction. The main beam is now reduced by 0.003 dB, and the largest grating lobe is in the $\phi=90^\circ$ -plane at $\theta = 1.3^\circ$ ($v=.023$) with a peak of 18.9 dBi, which is only 48 dB below the main peak. The most important grating lobes are shown in the pattern cuts in Figure 3-4b in the $\phi=0^\circ$ and 90° planes. The S_ℓ distance in the $\phi = 0^\circ$ plane varies from 70 mm to 120 mm giving the grating lobe distance of $\theta = 2.1^\circ$. In the $\phi = 90^\circ$ plane the S_ℓ distance is 72 mm which agrees very well with the θ value of 1.3° .

If the core print through peak is reduced to 2μ the grating lobes are again reduced by 14 dB as shown in Figure 3-5.

The GO approach on a distorted mirror is known to be inaccurate when the surface degradations are above a certain level. Therefore, the RF performance with 10μ dimpling on the secondary mirror is recalculated using PO on the secondary mirror. The patterns are shown in Figure 3-6. The shape of the contour lines is nearly the same as on the pattern in Figure 3-1a from the GO-PO calculation, but the grating lobe directions are slightly changed especially outside the symmetry plane. This is also to be seen in the pattern cuts in Figure 3-6b where the $\phi=90^\circ$ cut is no longer going through the lobe maxima.

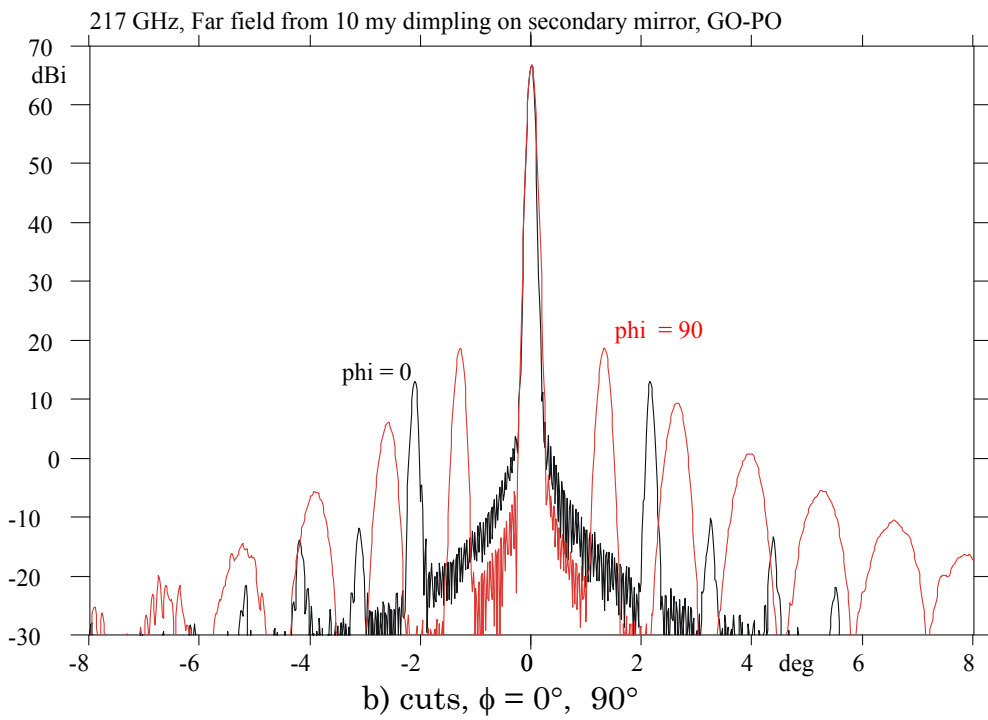
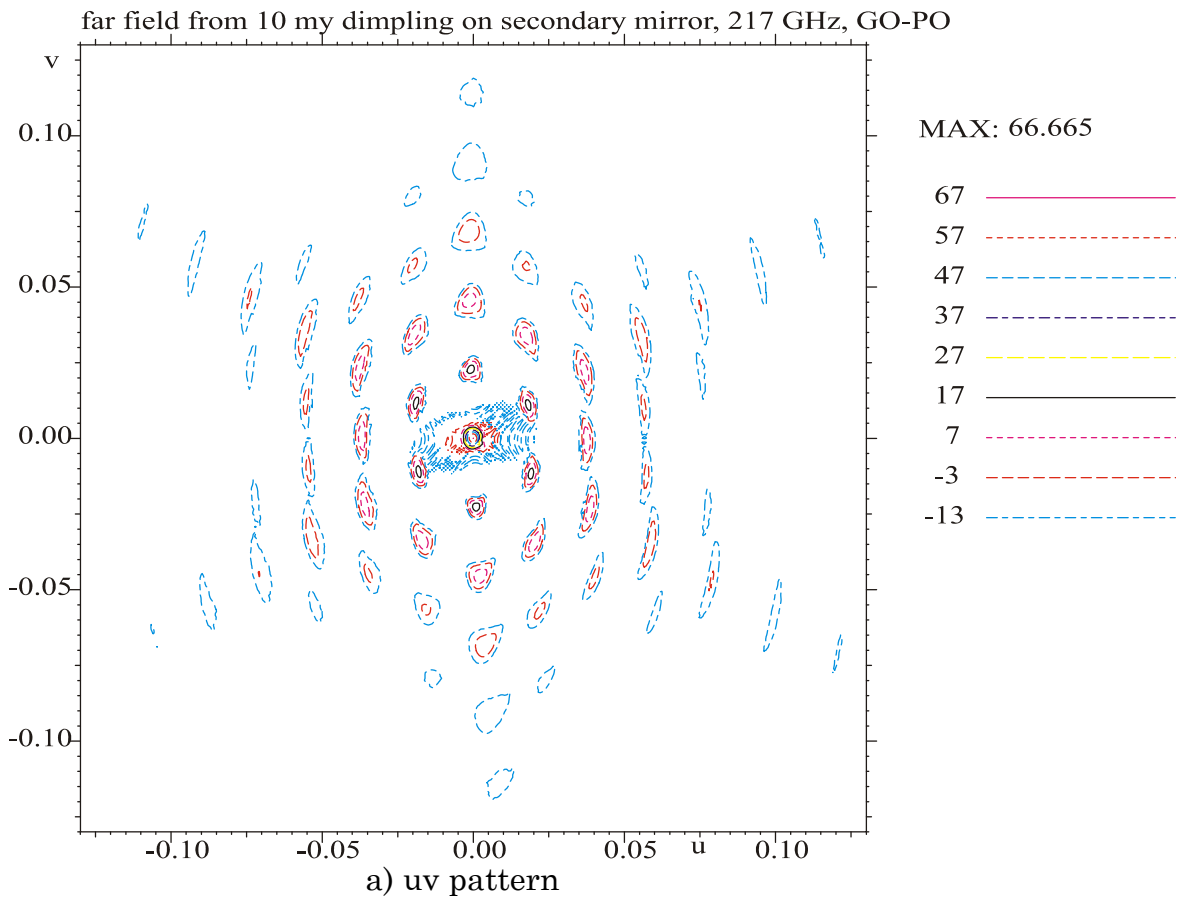


Figure 3-4 Far field from dimpling with 10 μ peak on secondary mirror. GO-PO

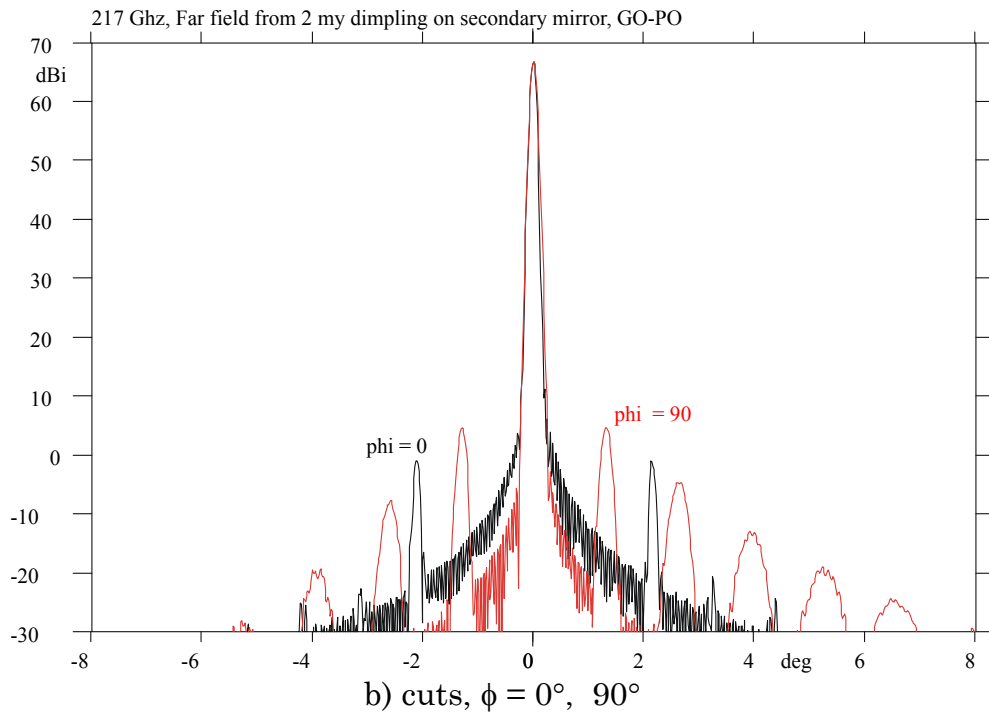
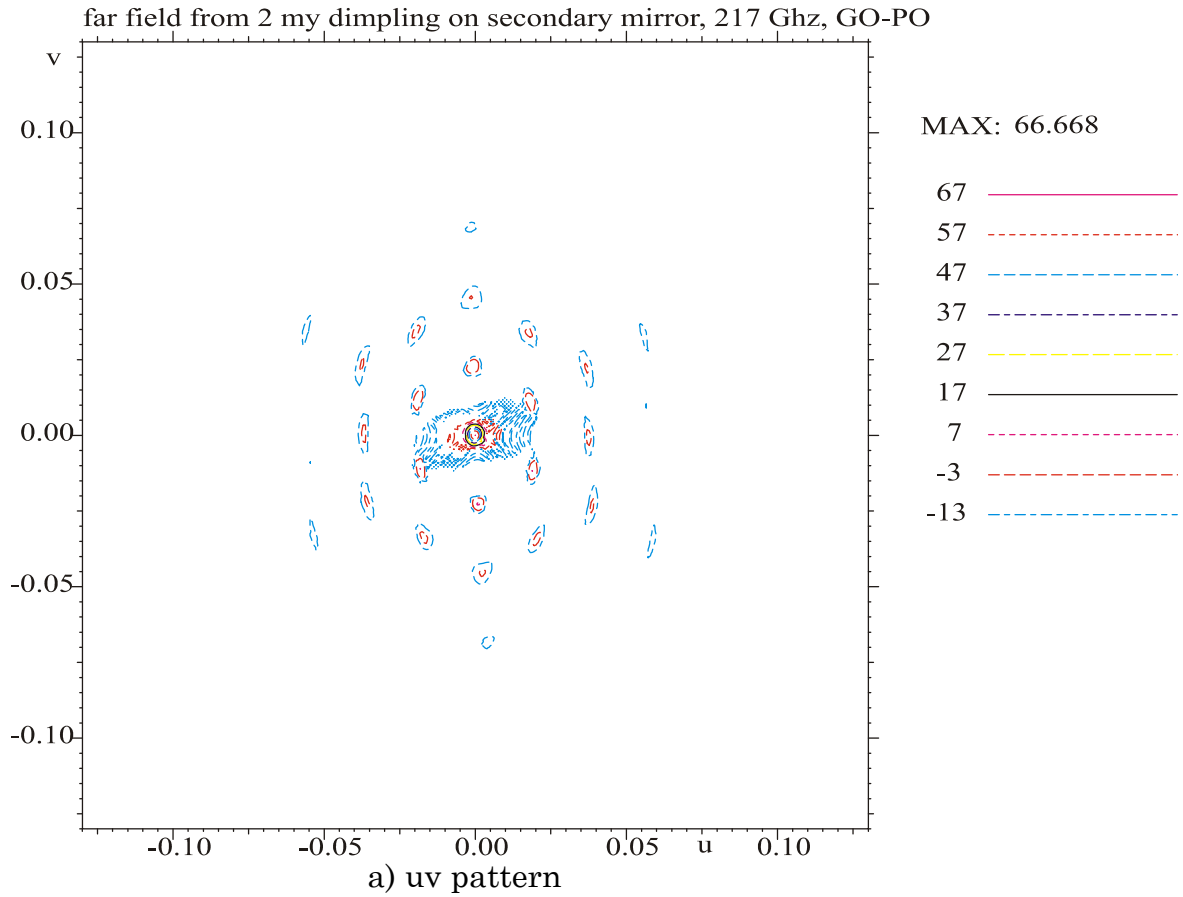


Figure 3-5 Far field from dimpling with 2 μ peak on secondary mirror. GO-PO

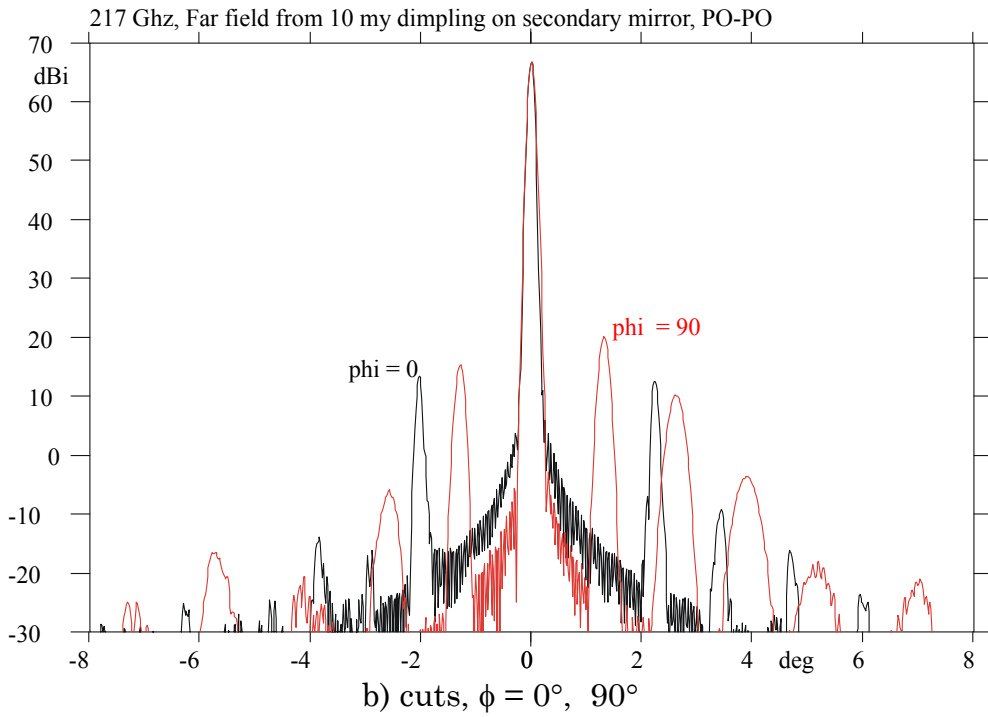
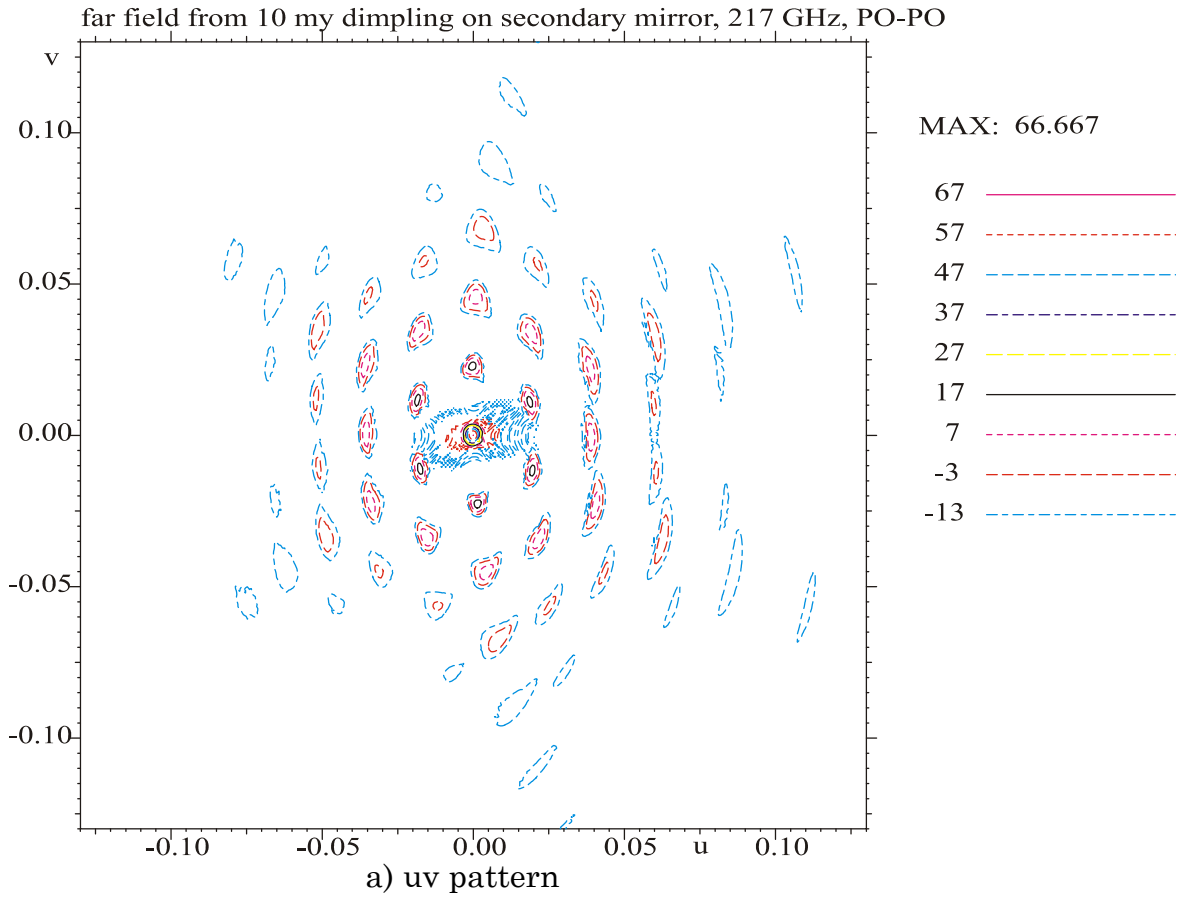


Figure 3-6 Far field from dimpling with 10 μ peak on secondary mirror. PO-PO

3.3 Distortions on primary and secondary mirror

The total far field from the 10 μ dimpling on both the primary and the secondary mirror is calculated using PO on both mirrors and is shown in Figure 3-7a. The contour lines are the same as on Figure 3-3a and Figure 3-6a, but the main beam is now reduced by 0.006 dB, which is the sum of the two beam reductions for distortions on the separate mirrors. The levels of the grating lobe are also the same as shown in the pattern cuts in Figure 3-7b.

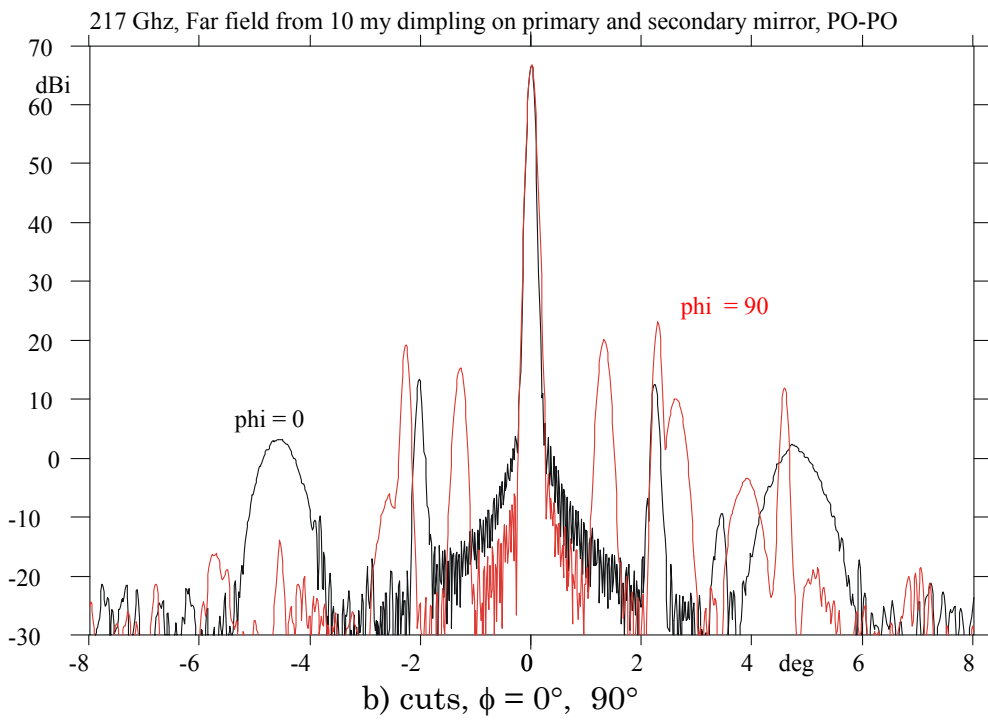
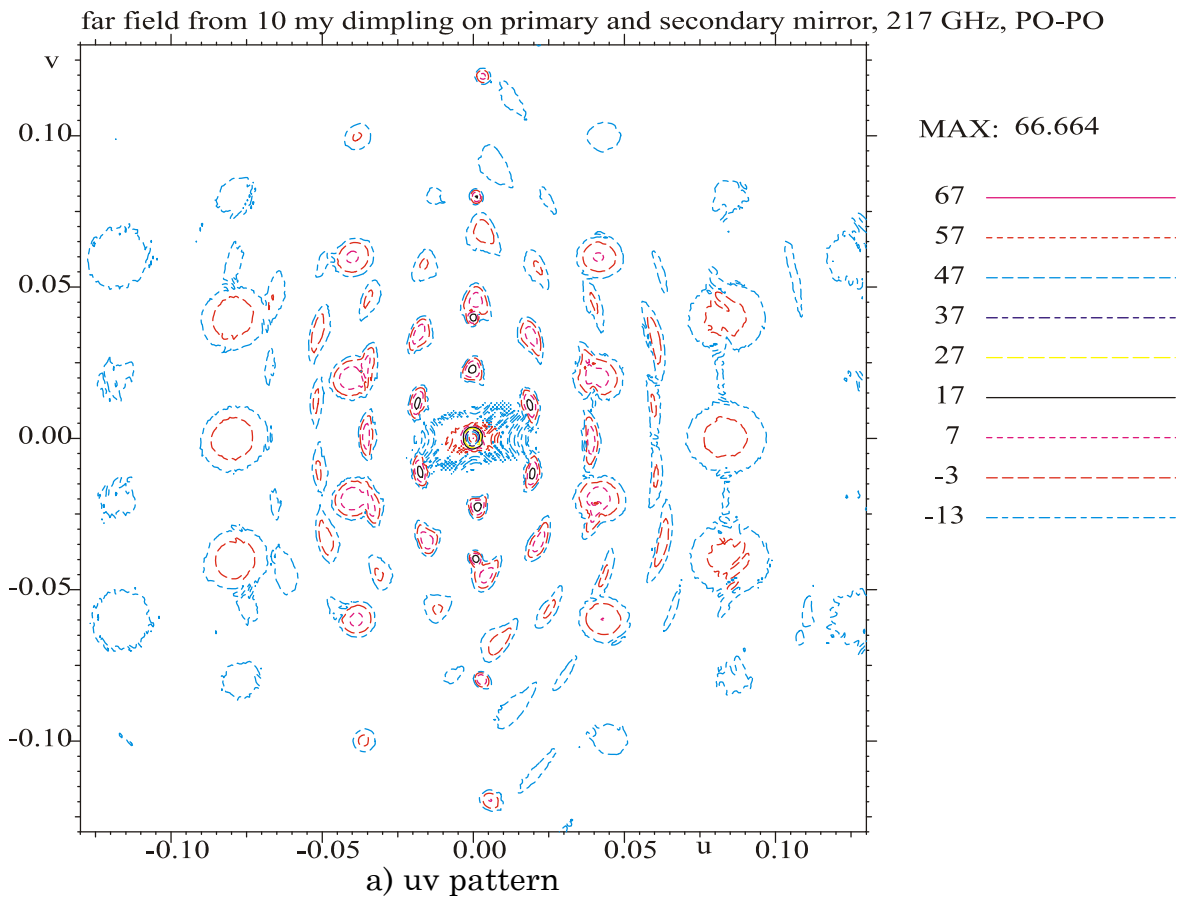


Figure 3-7 Far field from dimpling with 10 μ peak on both primary and secondary mirror. PO-PO

4. Frequency dependence

At other frequencies the direction of the grating lobes can be found using the equations (3.1) and (3.2), and the lobe closest to the main beam can be estimated by:

$$f_{\text{GHz}} * \sin(\theta_{\text{gr}}) \approx 8.7 \quad \text{for primary mirror distortion} \quad (4.1)$$

and

$$f_{\text{GHz}} * \sin(\theta_{\text{gr}}) \approx 4.9 \quad \text{for secondary mirror distortion} \quad (4.2)$$

where f_{GHz} is the frequency in GHz. The equations are checked in Table 4-1 using the old results for 857 GHz in Report S-801-05.

Frequency	217 GHz		857 GHz	
	primary	secondary	primary	secondary
Mirror with distortion				
Calculated by GRASP	2.3°	1.3°	0.58°	0.33°
Estimated by equation (4.1) and (4.2)	2.3°	1.3°	0.58°	0.33°

Table 4-1 θ angle of closest grating lobes

The phase degradation from the surface dimpling decreases linearly with the frequency. Therefore, the grating lobe levels will vary as

$$20.*\log(857/f_{\text{GHz}}) \text{ dB} \quad (4.3)$$

Therefore, the value of the first grating lobe amplitude below the main beam peak, ΔG_{gr} , at 10 μ dimpling on the primary mirror can be estimated by

$$\Delta G_{\text{gr}} = 32\text{dB} + 20.*\log(857/f_{\text{GHz}}) \text{ dB} \quad (4.4)$$

using the old results for 857 GHz and ΔG_{gr} from the secondary mirror is estimated by

$$\Delta G_{\text{gr}} = 33\text{dB} + 20.*\log(857/f_{\text{GHz}}) \text{ dB} \quad (4.5)$$

Due to different aperture illuminations and scan aberrations at the other frequencies there may be minor variations from these simple equations. The equations are checked in Table 4-2.

Frequency	217 GHz		857 GHz	
	primary	secondary	primary	secondary
Mirror with distortion				
Calculated by GRASP	43dB	48dB	32dB	33dB
Estimated by equation (4.4) and (4,5)	44dB	45dB	32dB	33dB

Table 4-2 grating lobe amplitude below the main beam peak

References

Alcatel (2001)

“Data interface status” ,Product code 22100,
H-P-3-ASPI-TN-0096, dated 06/09/01.

ESA (2000)

“Planck Telescope Design Specification”
SCI-PT-RS-07024, dated 31/08/00.

TICRA, 1999,

“RF properties of the Planck telescope, Designed by
ALCATEL CASE No. 1”. TICRA report S-801-04.

TICRA, 2000,

“RF effect of core print-through distortion on the Planck
telescope. TICRA report S-801-05.